AIAA Guidance, Navigation, and Control Conference
13 - 16 August 2012, Minneapolis, Minnesota

AIAA 2012-4620

Direct Fuzzy Adaptive Control of a Manipulator with Elastic Joints

Steve Ulrich[1] and Jurek Z. Sasiadek[2]
Carleton University, Ottawa, Ontario, K1S 5B6, Canada

The use of harmonic drive gear boxes in space robotic applications offer several attractive properties, such as high reduction ratio, compact size, low mass, and coaxial assembly. However, the flexibility effects of this type of gear mechanism in the joints of robotic manipulators are significant enough to make real-time control challenging. This paper addresses the problem of fuzzy adaptive trajectory control of space manipulators that exhibit elastic vibrations in their joints and that are subject to parametric uncertainties and dynamics modeling errors. The developed control scheme uses a fuzzy adaptation mechanism that varies in real-time the gains of a slow control term designed to stabilize the rigid dynamics, and a linear correction term to further reduce the elastic vibrations at the joints. The proposed controller is validated in numerical simulations in a trajectory tracking scenario by a flexible-joint manipulator. Simulation results suggest that the controller is robust to uncertainties in joint stiffness coefficients and to modeling errors, and yields improved tracking performance compared with conventional flexible-joint control strategies.

I. Introduction

THE benefits of lightweight space robotic manipulators are gained at the expense of higher elasticity in the joints. This leads to a more complex dynamic behavior. The additional flexible dynamics introduce two more state variables for each joint, which implies that the description of the complete dynamics model (including joint elasticity) requires four states for each joint: position and velocity of the motor rotor and position and velocity of the link. As a result, accelerating and stopping the arm produces large vibrations, making positioning of the end-effector very difficult. Achieving accurate motion and dampening elastic vibrations thus require advanced control techniques. Conventional model-based control strategies for flexible-joint manipulators, such as nonlinear feedback control,[1] and feedback linearization,[2] require good knowledge of the plant in the form of a mathematical model and its parameters. Consequently, if significant or unpredictable plant parameter variations arise, or if there are modeling errors due to complex flexible dynamics behaviors, model-based control approaches may perform inadequately. Although indirect adaptive control techniques may be used to estimate unknown plant parameters upon which the controller gains are obtained using some design procedure, this class of adaptive control methodologies nevertheless requires good knowledge of the dynamics model.[3] For example, Cao and de Silva[4] use an indirect adaptive control scheme in which neural networks approximate the unknown manipulator inertia and centrifugal-Coriolis matrices that are used explicitly in their control law. Alternatively, direct adaptive control techniques, with the controller gains updated directly in response to tracking errors, without requiring estimation of unknown plant parameters or mathematical models of the system to be controlled, can be used to address this problem.[5]

Ulrich et al.[6] developed an adaptive composite control strategy using the singular perturbation-based (SPB) theory, in which a slow direct adaptive control term is added to a fast control term designed to dampen the elastic vibrations at the joints of a flexible-joint manipulator system. The direct adaptive control system was based on the modified simple adaptive control (MSAC) methodology, using the tracking errors between the ideal system and the actual system outputs to adapt the controller gains.

In addition to direct adaptive control, fuzzy logic techniques have also been successfully applied to situations where mathematical modeling of the plant was uncertain; with flexible-joint manipulators for example. Goulet et al.[7] applied a complex multi-layer approach with a conventional control bottom layer, with a preprocess layer and an

[1] Ph.D. Candidate, Department of Mechanical and Aerospace Engineering, 1125 Colonel By Drive, Member AIAA.
[2] Professor, Department of Mechanical and Aerospace Engineering, 1125 Colonel By Drive, Associate Fellow AIAA.

intelligent fuzzy logic top layer, to a two-link flexible-joint manipulator, composed of revolute and prismatic joints. Ahmad et al.[8] used a fuzzy logic control system with triangular membership functions, to vary the input voltage of the robot's actuator, in response to the end-effector position errors and change-of-errors for a linearized state-space model of a single-link flexible-joint manipulator. The performance of this fuzzy control scheme, combined with an input shaping technique, was evaluated in numerical simulations in a set-point control scenario. Park and Cho[9] designed a fuzzy model reference adaptive control strategy and applied it to a single-link elastic-joint manipulator that was mathematically modeled by a Takagi-Sugeno fuzzy model. The design of this controller was based on the TS dynamics model using a parallel distributed compensation technique. Poor performance were achieved when tracking a sine-wave trajectory described in terms of joint angles, as demonstrated by the ±2 degree oscillating tracking error along the desired trajectory. Weiming et al.[10] proposed a fuzzy proportional-integral controller, with the joint angular position and velocity errors chosen as inputs, and an incremental control torque vector selected as the controller output. The control strategy included an inner-loop system that managed the variation of the incremental control gain, which significantly increased the complexity of the control scheme, largely due to the real-time numerical integration of various signals.

The purpose of this work is to address the problem of trajectory tracking by a two-link flexible-joint manipulator which is subject to large parametric uncertainties and modeling errors. The proposed strategy employs automatic tuning of the controller, enabling it to adapt to different plant conditions. To achieve this, a composite controller which uses a direct fuzzy adaptive control law as the slow control term is proposed. Within this context, the main contributions of this work are as follows. First, the strategy uses a novel direct adaptation mechanism based on fuzzy logic that adjusts the gains of the slow control term to yield good trajectory tracking performance in the presence of adverse conditions. This is, to the best of our knowledge, the first time a fuzzy logic approach is employed in a composite control scheme for flexible-joint robot manipulators. Second, as opposed to the previously mentioned existing flexible-joint control schemes, this new direct fuzzy adaptive method does not rely on on-line identification of plant parameters, is simple to implement, and renders effective trajectory-tracking performance regardless of large parametric uncertainties and dynamics modeling errors. Third, most existing control schemes for flexible-joint manipulators have been validated in numerical simulations using only the classic linear joint stiffness dynamics model.[11] In this work, similar to Ulrich et al.,[6] the performance of the proposed control strategy will also be assessed with a comprehensive dynamics model that captures nonlinear effects observed in experiments, such as friction and nonlinear joint stiffness. This nonlinear model will be used as a mean to validate the robustness of the proposed controller to modeling errors.

II. Elastic-Joint Manipulator Dynamics

Consider a class of two-link elastic-joint robot manipulator systems, whose nonlinear dynamics is derived in terms of kinetic and potential energies stored in the system by the Euler–Lagrange formulation. Assuming that each joint is modeled as a linear torsional spring of constant stiffness, the resulting dynamics of flexible-joint manipulators with revolute joints which are actuated directly by DC motors are represented by the following second-order differential equations[11]

$$\mathbf{M}(\mathbf{q})\ddot{\mathbf{q}} + \mathbf{C}(\mathbf{q},\dot{\mathbf{q}})\dot{\mathbf{q}} - \mathbf{k}(\mathbf{q}_m - \mathbf{q}) = \mathbf{0} \tag{1}$$

$$\mathbf{J}_m\ddot{\mathbf{q}}_m + \mathbf{k}(\mathbf{q}_m - \mathbf{q}) = \boldsymbol{\tau} \tag{2}$$

where $\mathbf{M}(\mathbf{q}) \in \mathbb{R}^{2\times 2}$ denotes the symmetric and positive-definite inertia matrix, $\mathbf{C}(\mathbf{q},\dot{\mathbf{q}}) \in \mathbb{R}^{2\times 2}$ denotes the centrifugal-Coriolis matrix, $\boldsymbol{\tau}(t) \in \mathbb{R}^2$ denotes the control torque vector, $\mathbf{q}(t)$, $\dot{\mathbf{q}}(t)$, $\ddot{\mathbf{q}}(t) \in \mathbb{R}^2$ represent the link position, velocity and acceleration vector respectively, $\mathbf{q}_m(t)$, $\dot{\mathbf{q}}_m(t)$, $\ddot{\mathbf{q}}_m(t) \in \mathbb{R}^2$ denote the motor position, velocity and acceleration vector respectively, $\mathbf{J}_m \in \mathbb{R}^{2\times 2}$ denotes the positive-definite motor inertia matrix, and $\mathbf{k} \in \mathbb{R}^{2\times 2}$ represents the diagonal positive-definite stiffness matrix of the joints.

In the following, it is assumed that the Euler-Lagrange system defined in Eqs. (1) and (2) is fully-actuated and non-redundant, and that the Jacobian matrix denoted by $\mathbf{J}(\mathbf{q}) \in \mathbb{R}^{2\times 2}$ has full rank column. Thus, holonomic constraints can be selected in order for the generalized link positions and velocities to satisfy the relation

$$\begin{bmatrix} \dot{x}_p(t) \\ \dot{y}_p(t) \end{bmatrix} = \mathbf{J}(\mathbf{q})\dot{\mathbf{q}}(t) \tag{3}$$

where $\dot{x}_p(t)$, $\dot{y}_p(t) \in \mathbb{R}$ denote the end-effector Cartesian velocity along the *x* and *y* axes, respectively. Similarly, it is assumed that there exists a mapping allowing the Cartesian position of the end-effector with respect to the robot reference frame along both axes to be obtained as

$$\begin{bmatrix} x_p(t) \\ y_p(t) \end{bmatrix} = \Omega(\mathbf{q}) \tag{4}$$

where $\Omega(\mathbf{q}) \in \mathbb{R}^2$ is the forward kinematic transformation taking the link positions into end-effector Cartesian position. By combining (3) and (4), joint-space variables are transformed into the task-space (Cartesian) manipulator system output vector $\mathbf{y}_p(t) \in \mathbb{R}^4$ through the transformation[12]

$$\mathbf{y}_p(t) = \begin{bmatrix} x_p \\ y_p \\ \dot{x}_p \\ \dot{y}_p \end{bmatrix} = \begin{bmatrix} l_1 \cos(q_1) + l_2 \cos(q_1 + q_2) \\ l_1 \sin(q_1) + l_2 \sin(q_1 + q_2) \\ -l_1 \sin(q_1)\dot{q}_1 - l_2 \sin(q_1 + q_2)(\dot{q}_1 + \dot{q}_2) \\ l_1 \cos(q_1)\dot{q}_1 + l_2 \cos(q_1 + q_2)(\dot{q}_1 + \dot{q}_2) \end{bmatrix} \tag{5}$$

where $l_i \ \forall i = 1,2$ denote the length of the *i*th link.

III. Problem Statement

The objective is to design a fuzzy adaptive controller which ensures that the flexible-joint robot manipulator tracks the output vector $\mathbf{y}_m(t)$ of the following reference model

$$\dot{\mathbf{x}}_m(t) = \mathbf{A}_m \mathbf{x}_m(t) + \mathbf{B}_m \mathbf{u}_m(t) \tag{6}$$

$$\mathbf{y}_m(t) = \mathbf{C}_m \mathbf{x}_m(t) \tag{7}$$

where

$$\mathbf{y}_m(t) = \begin{bmatrix} x_m \\ y_m \\ \dot{x}_m \\ \dot{y}_m \end{bmatrix} \in \mathbb{R}^4, \qquad \mathbf{u}_m(t) = \begin{bmatrix} x_d \\ y_d \\ \dot{x}_d \\ \dot{y}_d \end{bmatrix} \in \mathbb{R}^4 \tag{8}$$

are the reference model outputs and inputs respectively, and where x_m, y_m, $\dot{x}_m$, $\dot{y}_m \in \mathbb{R}$, denote the ideal closed-loop position and velocity response to the desired position and velocity of the robot end-effector, denoted by x_d, y_d, $\dot{x}_d$, $\dot{y}_d \in \mathbb{R}$, respectively. The reference model was selected to incorporate the desired input–output plant behavior, and is not based on any modeling of the plant. It is expressed in terms of the ideal damping ratio $\zeta \in \mathbb{R}$, and undamped natural frequency $\omega_n \in \mathbb{R}$, as follows

$$\mathbf{A}_m = \begin{bmatrix} 0 & 0 & 0 & 0 \\ 0 & 0 & 0 & 0 \\ -\omega_n^2 & 0 & -2\zeta\omega_n & 0 \\ 0 & -\omega_n^2 & 0 & -2\zeta\omega_n \end{bmatrix} \qquad \mathbf{B}_m = \begin{bmatrix} 0 & 0 & 1 & 0 \\ 0 & 0 & 0 & 1 \\ \omega_n^2 & 0 & 0 & 0 \\ 0 & \omega_n^2 & 0 & 0 \end{bmatrix} \qquad \mathbf{C}_m = I_4 \tag{9}$$

To quantify the control objective, an output tracking error vector, denoted by $\mathbf{e}_y(t) \in \mathbb{R}^4$, is defined as

$$\mathbf{e}_y(t) \triangleq \mathbf{y}_m - \mathbf{y}_p = \begin{bmatrix} x_e \\ y_e \\ \dot{x}_e \\ \dot{y}_e \end{bmatrix} \tag{10}$$

IV. Fuzzy Adaptive Control Development

Similar to the recently developed MSAC-based direct adaptive control method,[6] the proposed control strategy uses the singular perturbation-based (SPB) theory, which transforms a dynamic model into a two-timescale model: the quasi-steady-state model and the boundary-layer model. When applied to flexible-joint manipulators, the SPB theory provides a framework for the design of composite controllers, in which the motor torque control input is given by $\boldsymbol{\tau} = \boldsymbol{\tau}_s + \boldsymbol{\tau}_f$, where subscript *s* stands for slow variables defined in the slow time scale *t*, and the subscript *f* stands for variables defined in the fast time scale $t' = t/\epsilon$, with $\epsilon \in \mathbb{R}$ as a small positive parameter. Following common practice, the slow control torque $\boldsymbol{\tau}_s$ is designed to stabilize the quasi-steady-state model (which has a form equivalent to the rigid-joint dynamics model), and the fast-control torque $\boldsymbol{\tau}_f$ is applied to the boundary-layer model. This control torque separation approach inherent to the SPB theory results in an important practical design consideration regarding the slow control term[13]: it must be function of the state of the quasi-steady state model, and must not contain a feedback of the control torque. As a result, not any rigid-joint controllers may be considered as the slow control term. A more detailed treatment of the SPB theory can be found in Khalil's work.[14] The composite control law proposed herein that satisfies the consideration stated above is given by

$$\boldsymbol{\tau} = \mathbf{J}^T(\mathbf{q})\mathbf{K}_e(t)\mathbf{e}_y + \mathbf{K}_v(\dot{\mathbf{q}} - \dot{\mathbf{q}}_m) \tag{11}$$

where $\mathbf{J}^T(\mathbf{q})\mathbf{K}_e(t)\mathbf{e}_y$ represents the slow control term and $\mathbf{K}_v(\dot{\mathbf{q}} - \dot{\mathbf{q}}_m)$ represents the fast control term. In Eq. (11), $\mathbf{K}_v \in \mathbb{R}^{2\times 2}$ is a fixed control gain matrix, and $\mathbf{K}_e(t) \in \mathbb{R}^{2\times 4}$ is a time-varying control gain matrix that maintains satisfactory trajectory tracking performance. Note that the fast control term provides additional damping of the elastic vibrations at the joints, but does not cancel them completely. Therefore, unlike conventional rigid-joint controllers, the slow control term must be effective enough to cope with any residual vibrations of the end-effector motion, which are fed back via the trajectory tracking error signal $\mathbf{e}_y$.

Alternatively, $\mathbf{K}_e(t)$ can be defined in terms of a time-varying proportional $\mathbf{K}_p(t) \in \mathbb{R}^{2\times 2}$ and derivative control gain $\mathbf{K}_d(t) \in \mathbb{R}^{2\times 2}$, as follows

$$\mathbf{K}_e(t) \triangleq \begin{bmatrix} \mathbf{K}_p(t) & \mathbf{K}_d(t) \end{bmatrix} \tag{12}$$

Adaptation of these control gains is achieved via a fuzzy logic mechanism, which updates the gains as a function of the tracking errors between the actual plant outputs and the reference model outputs. Adopting a decentralized approach, $\mathbf{K}_p(t)$ and $\mathbf{K}_d(t)$ are adapted as follows

$$\mathbf{K}_p(t) = \mathrm{diag}\{\lambda_1(t)h_1, \lambda_2(t)h_2\} \tag{13}$$

$$\mathbf{K}_d(t) = \mathrm{diag}\{\lambda_3(t)h_3, \lambda_4(t)h_4\} \tag{14}$$

where the time-varying control parameters $\lambda_q \in \mathbb{R}\ \forall q = 1,\ldots 4$, represent the defuzzified outputs of a normalized fuzzy logic system (FLS). As shown in Eqs. (13) and (14), each λ_q is dedicated to the control of a single element of the tracking error vector along a single axis, resulting in a decentralized approach. More specifically, the proportional-based control parameters λ_1 and λ_2 are applied to the position tracking errors x_e and y_e respectively, whereas the derivative-based control parameters λ_3 and λ_4 are applied to the velocity tracking errors $\dot{x}_e$ and $\dot{y}_e$ respectively. Whenever possible, the adaptation mechanism of each control parameter is based on its associated tracking error and its time-derivative. Thus, since no acceleration measurements are assumed, the adaptation mechanism of λ_3 and λ_4 are based only on $\dot{x}_e$ and $\dot{y}_e$ respectively. Figure 1 illustrates the block scheme implementation of the direct fuzzy adaptive system, where each component is described in the following subsections. Unlike existing fuzzy-logic control methodologies for flexible-joint manipulators, [7-10] the proposed strategy does not output the defuzzified control input signals, but rather outputs time-varying control parameters which are used to update the control gains in response to the trajectory tracking errors, thus resulting in a direct adaptive control scheme.

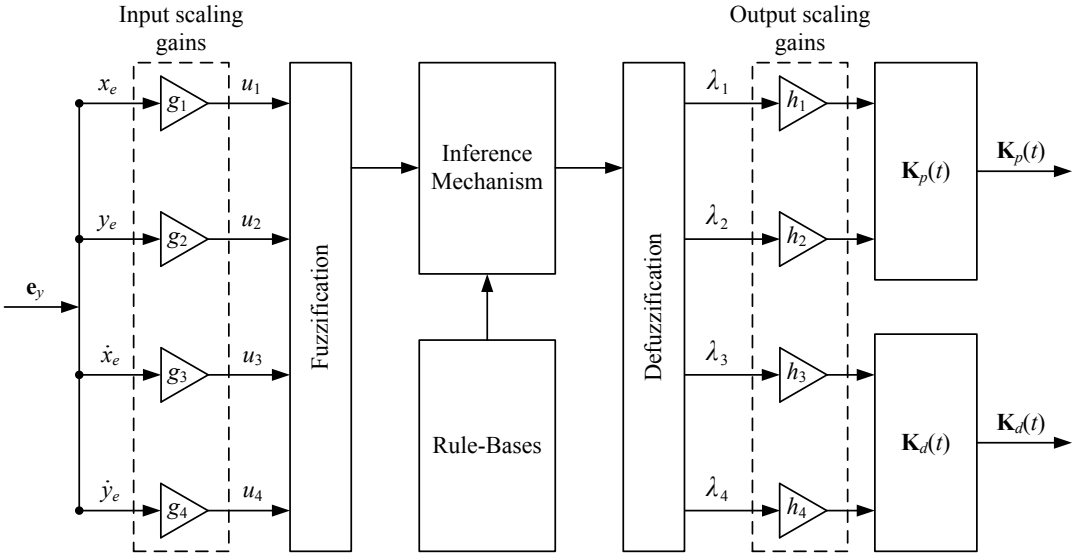

Fig. 1 Block scheme diagram of direct fuzzy adaptation mechanism implementation.

A. Fuzzification

The universes of discourse are ± 2/3 m for x_e and y_e, ±10 m/s for $\dot{x}_e$ and $\dot{y}_e$, and 0 to 1 for λ_q. The input scaling gains $g_i \in \mathbb{R}$, are selected as $g_1 = g_2 = 1.5$ and $g_3 = g_4 = 0.1$, so that the universe of discourse U_i for the normalized crisp inputs $u_i \in U_i\ \ \forall i = 1,\ldots 4$, are defined in $U_i = [-1\ \ 1]$. Constant linguistic variables denoted by $\tilde{u}_i$ and $\tilde{\lambda}_q$, are used to describe the time-varying crisp inputs u_i and outputs λ_q, respectively. Here, $\tilde{u}_1 = $ *position error along the x-axis*, $\tilde{u}_2 = $ *position error along the y-axis*, $\tilde{u}_3 = $ *velocity error along the x-axis*, $\tilde{u}_4 = $ *velocity error along the y-axis*, $\tilde{\lambda}_1 = $ *proportional-based control parameter along the x-axis*, $\tilde{\lambda}_2 = $ *proportional-based control parameter along the y-axis*, $\tilde{\lambda}_3 = $ *derivative-based control parameter along the x-axis*, and $\tilde{\lambda}_4 = $ *derivative-based control parameter along the y-axis*. In turn, linguistic variables $\tilde{u}_i$ take on elements from the set of nine linguistic values denoted by $\tilde{A}_i = \left\{\tilde{A}_i^j : i = 1,\ldots 4 : j = 1,\ldots 9\right\}$, where $\tilde{A}_i^j$ denotes the j^{th} linguistic value. Similarly, $\tilde{B}_i^j\ \ \forall i = 1,2$ denotes the j^{th} linguistic value for linguistic variables $\tilde{\lambda}_1$ and $\tilde{\lambda}_2$, both of which take on elements from

the set of nine linguistic values denoted by $\widetilde{B}_{1,2} = \left\{\widetilde{B}_i^j : i = 1,2 : j = 1,\ldots 9\right\}$, and $\widetilde{B}_i^j \ \forall i = 3,4$ denotes the j^{th} linguistic value for linguistic variables $\widetilde{\lambda}_3$ and $\widetilde{\lambda}_4$ which both take on elements from the set of five linguistic values denoted by $\widetilde{B}_{3,4} = \left\{\widetilde{B}_i^j : i = 3,4 : j = 1,\ldots 5\right\}$. Based on Green and Sasiadek,[15] linguistic values are defined as *negative very high* (NVH), *negative high* (NH), *negative low* (NL), *negative very low* (NVL), *zero* (ZERO), *positive very very low* (PVVL), *positive very low* (PVL), *positive low* (PL), *positive medium* (PM), *positive high* (PH), *positive very high* (PVH), *positive very very high* (PVVH), and *positive maximum* (PMAX).

Through fuzzification, crisp input u_i are first mapped into fuzzy sets denoted by A_i^j, and defined as

$$A_i^j = \left\{(u_i, \mu_{A_i^j}(u_i)) : u_i \in U_i\right\} \quad i = 1,\ldots,4 \quad j = 1,\ldots,9 \tag{15}$$

where the membership function $\mu_{A_i^j}(u_i)$ associated with $\widetilde{A}_i^j$ maps U_i to [0 1], in order to determine the degree of certainty that u_i with linguistic description $\widetilde{u}_i$ may be classified linguistically as $\widetilde{A}_i^j$. All input u_i and output variables λ_q are designed with Gaussian membership functions. It is notable that, unlike triangular or trapezoidal functions, Gaussian membership functions render non-zero degrees of membership over the entire universe of discourse. In this study, input Gaussian membership functions are modeled as

$$\mu_{A_i^j}(u_i) = e^{-\frac{1}{2}\left(\frac{u_i - c_{A_i^j}}{\sigma_{A_i^j}}\right)^2} \quad i = 1,\ldots,4 \quad j = 1,\ldots,9 \tag{16}$$

where $c_{A_i^j}$, $\sigma_{A_i^j} \in \mathbb{R}$ represent the center and width (shape) of the functions respectively. Output Gaussian membership functions $\mu_{B_i^j}(\lambda_q)$ are also described mathematically using the same model. The resulting membership functions for input and output variables are provided in Figs. 2 to 4. Note that these membership functions are defined for normalized input and output variables, suggesting that the left-most membership functions saturate (peak) at -1, and the right-most at +1.

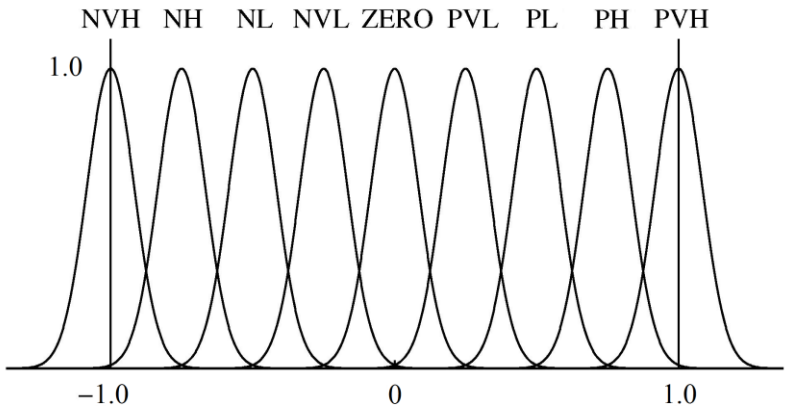

Fig. 2 Membership functions for normalized input variables u_1, u_2, u_3 and u_4.

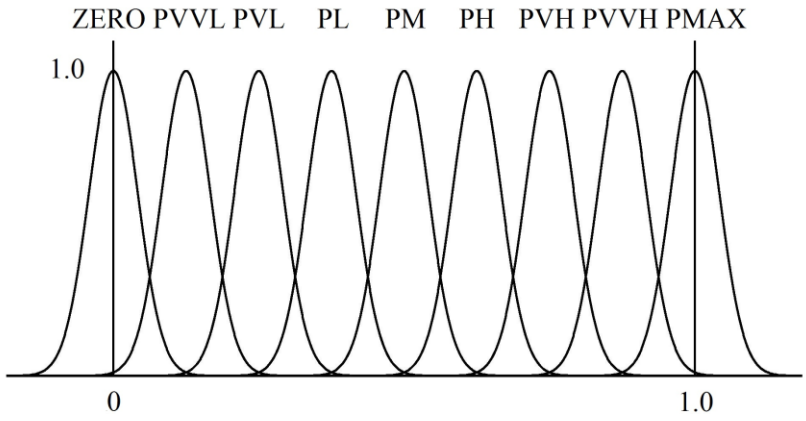

Fig. 3 Membership functions for normalized output variables λ_1 and λ_2.

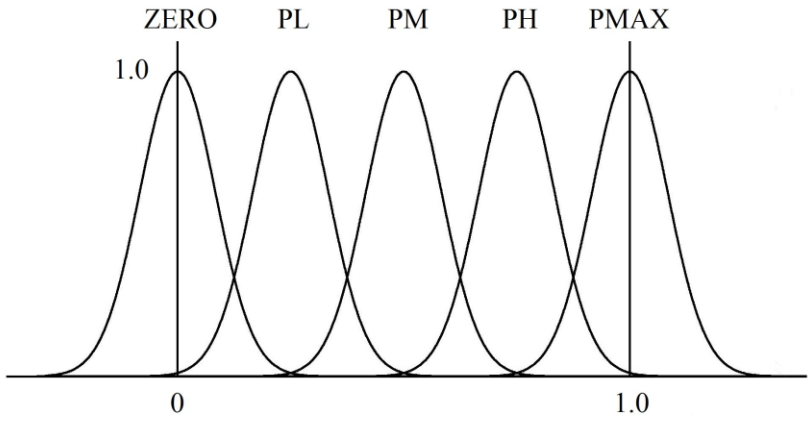

Fig. 4 Membership functions for normalized output variables λ_3 and λ_4.

B. Rule-Bases

The previously-defined linguistic values are also used to generate linguistic rules of the form

IF $\tilde{u}_1$ is NH **AND** $\tilde{u}_3$ is PL **THEN** $\tilde{\lambda}_1$ is PH

IF $\tilde{u}_2$ is PVL **AND** $\tilde{u}_4$ is NL **THEN** $\tilde{\lambda}_2$ is PL

IF $\tilde{u}_3$ is PVH **THEN** $\tilde{\lambda}_3$ is PMAX

IF $\tilde{u}_4$ is NL **THEN** $\tilde{\lambda}_4$ is PM

The rules are designed intuitively; as the magnitude of a given tracking error along an axis varies positively or negatively, the associated control parameter λ_q varies accordingly. The values of λ_q are maintained ≥ 0, ranging from ZERO for zero tracking errors to PMAX for the largest tracking errors, either positive or negative. As mentioned, the adaptation of λ_1 and λ_2 is also based on the magnitude of velocity tracking errors, and varies accordingly. The resulting symmetric rule matrices are given in Tables 1 and 2.

Table 1. Fuzzy logic system rule table for $\tilde{\lambda}_1$ and $\tilde{\lambda}_2$.

$\{\tilde{\lambda}_1, \tilde{\lambda}_2\}$		$\{\tilde{u}_1, \tilde{u}_2\}$								
		NVH	**NH**	**NL**	**NVL**	**ZERO**	**PVL**	**PL**	**PH**	**PVH**
$\{\tilde{u}_3, \tilde{u}_4\}$	**NVH**	PMAX	PMAX	PVH	PH	PM	PH	PVH	PMAX	PMAX
	NH	PMAX	PMAX	PH	PM	PL	PM	PH	PMAX	PMAX
	NL	PVH	PH	PM	PL	PVL	PL	PM	PH	PVH
	NVL	PH	PM	PL	PVL	PVVL	PVL	PL	PM	PH
	ZERO	PM	PL	PVL	PVVL	ZERO	PVVL	PVL	PL	PM
	PVL	PH	PM	PL	PVL	PVVL	PVL	PL	PM	PH
	PL	PVH	PH	PM	PL	PVL	PL	PM	PH	PVH
	PH	PMAX	PMAX	PH	PM	PL	PM	PH	PMAX	PMAX
	PVH	PMAX	PMAX	PVH	PH	PM	PH	PVH	PMAX	PMAX

Table 2. Fuzzy logic system rule table for $\tilde{\lambda}_3$ and $\tilde{\lambda}_4$.

$\{\tilde{u}_3, \tilde{u}_4\}$	**NVH**	**NH**	**NL**	**NVL**	**ZERO**	**PVL**	**PL**	**PH**	**PVH**
$\{\tilde{\lambda}_3, \tilde{\lambda}_4\}$	PMAX	PH	PM	PL	ZERO	PL	PM	PH	PMAX

C. Inference Mechanism

For rules involving two premise terms (i.e. rules with a consequent of either $\tilde{\lambda}_1$ or $\tilde{\lambda}_2$), the degree of certainty to which the i^{th} rule applies is quantified with the MIN operator, as follows

$$\mu_i(u_1, u_3) = \min\left\{\mu_{A_1^j}(u_1), \mu_{A_3^k}(u_3)\right\} \qquad i = 1,\ldots,81 \quad j = 1,\ldots,9 \quad k = 1,\ldots,9 \tag{17}$$

$$\mu_i(u_2, u_4) = \min\left\{\mu_{A_2^j}(u_2), \mu_{A_4^k}(u_4)\right\} \qquad i = 1,\ldots,81 \quad j = 1,\ldots,9 \quad k = 1,\ldots,9 \tag{18}$$

Otherwise, for rules with a consequent of either $\tilde{\lambda}_3$ or $\tilde{\lambda}_4$, the degree of certainty to which the i^{th} rule applies is simply obtained as

$$\mu_i(u_3) = \mu_{A_3^i}(u_3) \qquad i = 1,\ldots,9 \tag{19}$$

$$\mu_i(u_4) = \mu_{A_4^i}(u_4) \qquad i = 1,\ldots,9 \tag{20}$$

Next, the membership function $\mu_{B_q^i}(\lambda_q) \quad \forall q = 1,\ldots,4$ of the implied fuzzy set B_q^i for the i^{th} rule is computed with the MIN operator, as follows

$$\mu_{B_1^i}(\lambda_1) = \min\left\{\mu_i(u_1, u_3), \mu_{B_1^p}(\lambda_1)\right\} \qquad i = 1,\ldots,81 \tag{21}$$

$$\mu_{B_2^i}(\lambda_2) = \min\left\{\mu_i(u_2, u_4), \mu_{B_2^p}(\lambda_2)\right\} \qquad i = 1,\ldots,81 \tag{22}$$

$$\mu_{B_3^i}(\lambda_3) = \min\left\{\mu_i(u_3), \mu_{B_3^p}(\lambda_3)\right\} \qquad i = 1,\ldots,9 \tag{23}$$

$$\mu_{B_4^i}(\lambda_4) = \min\left\{\mu_i(u_4), \mu_{B_4^p}(\lambda_4)\right\} \qquad i = 1,\ldots,9 \tag{24}$$

where the implied fuzzy set B_q^i specifies the certainty level at which the q^{th} control parameter should be a specific crisp value, taking only rule *i* into consideration. The resulting membership function $\mu_{B_q^i}(\lambda_q)$ is a function of λ_q, and the MIN operator truncates the top of the $\mu_{B_q^p}(\lambda_q)$ membership function associated with the output fuzzy set B_q^p of the i^{th} rule. Since the MIN operator works on each point of a given output membership curve, the final shape of the implied membership function could change depending on the number of points used to generate the membership functions. In this study, each output membership function is modeled with 100 points, evenly distributed across the output universe of discourse.

As an alternative to using implied fuzzy sets to perform the inference step, the overall implied fuzzy set with membership function $\mu_{B_q}(\lambda_q)$, which represents the conclusion reached by all rules simultaneously, can be computed, as it was done in Ref. 15. However, as explained by Passino and Yurkovich,[16] the use of the overall implied fuzzy set is not recommended for real-time applications, due to the increased complexity in both the computation of the overall implied fuzzy set itself, and in the defuzzification step, which is usually based on the center of area (COA) method.

D. Defuzzification

The center of gravity (COG) defuzzification method calculates a crisp control parameter $\lambda_q \quad \forall q = 1,\ldots,4$ based on area and center-of-area of all implied fuzzy sets. Using this method, the crisp value for the control parameter λ_q is given by

$$\lambda_q = \frac{\sum_{i=1}^{n} b_i^q \int \mu_{B_q^i}(\lambda_q) d\lambda_q}{\sum_{i=1}^{n} \int \mu_{B_q^i}(\lambda_q) d\lambda_q} \qquad q = 1,\ldots,4 \tag{25}$$

where $n \in \mathbb{R}$ denotes the number of rules (81 for λ_1 and λ_2, and 9 for λ_3 and λ_4), and $b_i^q \in \mathbb{R}$ denotes the center of area of the membership function of B_q^p associated with the implied fuzzy set B_q^i for the i^{th} rule.

Output scaling gains $h_q \in \mathbb{R} \ \forall q = 1,\ldots 4$ multiply their corresponding control parameter λ_q, to modify the base widths and provide greater tracking accuracy as the scaling gains increase. Increasing output scaling gains spreads out the output membership functions, and makes the meaning of their associated linguistics quantify larger numbers.[16]

The resulting nonlinear adaptation surface and nonlinear adaptation curve that concisely represent all the information in the fuzzy adaptation mechanism are shown in Figs. 5 and 6 respectively. Note that decreasing the input scaling gains would rescale the axes and decrease the slope of the adaptation surface and adaptation curve, and the controller's overall sensitivity to small tracking errors. Conversely, setting the input scaling gains too high would make the membership functions saturate at low values, resulting in oscillations or chattering. The ripple effects observed in Figs. 5 and 6 are created by the interpolation between the different rules. Ultimately, tuning the scaling gains, selecting the membership functions, and defining the rules modifies the shape of the adaptation surface and adaptation curve, which in turn may affect the closed-loop behavior.

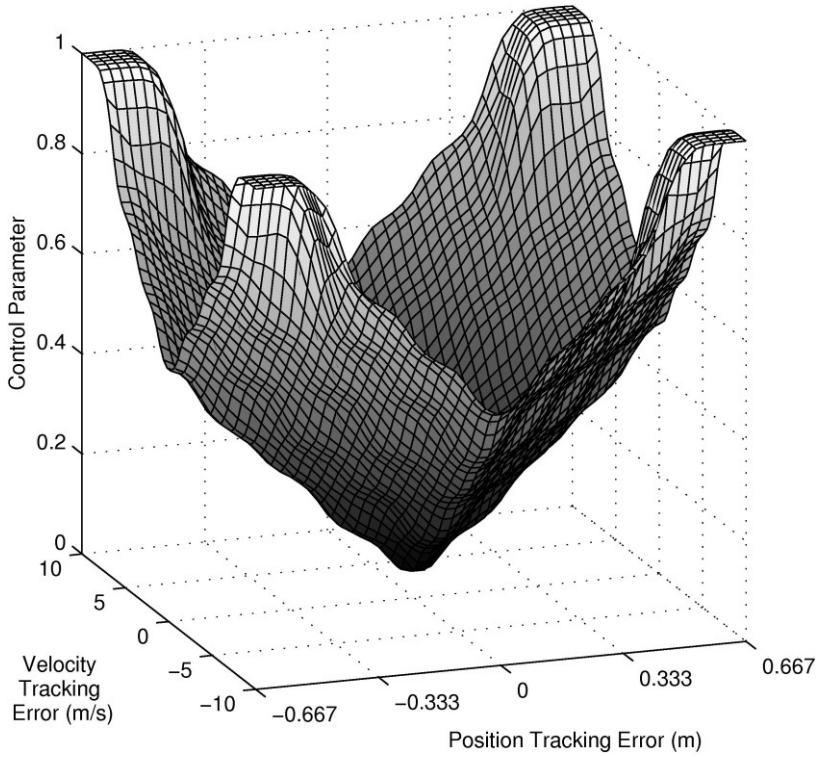

Fig. 5 Nonlinear adaptation surface for λ_1 and λ_2.

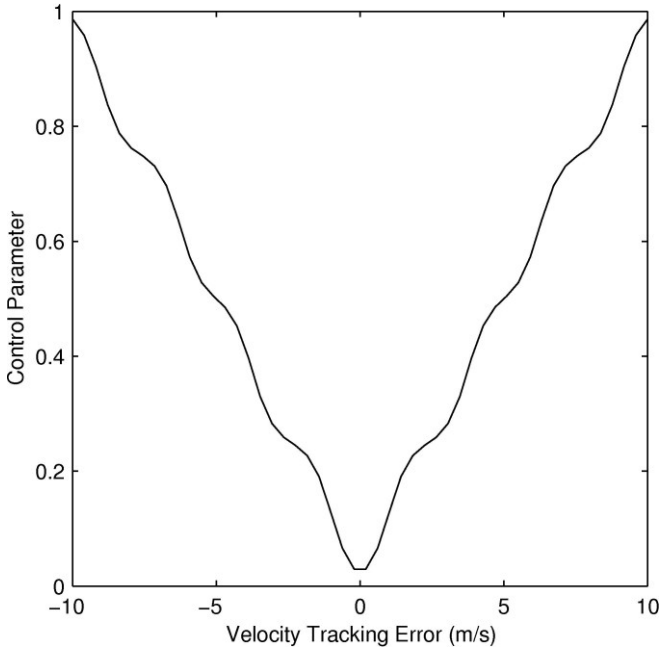

Fig. 6 Nonlinear adaptation curve for λ_3 and λ_4.

V. Numerical Simulations

This section presents the numerical simulation results obtained by implementing the direct fuzzy adaptive composite controller developed in this study. The parameters of the two-link flexible-joint manipulator are based on previous studies,[6,15,17] and are summarized as follows: $l_1 = l_2 = 4.5$ m, $m_1 = m_2 = 1.5075$ kg, $\mathbf{J}_m$ = diag[1] kg·m^2 and $\mathbf{k}$ = diag[500] N·m/rad. These unknown plant parameters have only been used to select the output scaling gains and the control gain matrix of the fast control term in numerical simulations. Good results with the linear robot manipulator were achieved with $h_1 = h_2 = 100$, $h_3 = h_4 = 270$ and $\mathbf{K}_v$ = diag[35] N·m·s/rad. The selected reference model parameters are ω_n = 10 rad/s and ζ = 0.9. Figures 7 and 8 show the trajectory-tracking results of a 12.6 × 12.6 m square trajectory by the nominal robot manipulator described previously, in 60 seconds in a counterclockwise direction starting from rest at the lower-right-hand corner. Such square trajectories to assess the trajectory-tracking performance of flexible space manipulators are common in the literature (see Refs. 6, 15, and 17 for examples).

The trajectory shown in Fig. 7 exhibits minimal overshoots of 0.089 m at each direction change, with rapid settling to a steady-state along each side of the trajectory. The corresponding time-varying control gains $\mathbf{K}_p(t)$ and $\mathbf{K}_d(t)$, shown in Fig. 8, are relatively low in magnitude and almost constant between two direction changes, and sharply increase when the end-effector reaches each corner of the square trajectory, thus adapting the control law to reduce tracking errors.

Numerical simulations using a robot with joints of significantly lower stiffness were performed in order to assess the robustness of the proposed controller to parametric uncertainties in the plant. The same composite controller tuned previously with the nominal robot manipulator was applied to a robot with a joint stiffness matrix of $\mathbf{k}$ = diag[200] N·m/rad, representing an uncertainty of 60%. The obtained results are shown in Fig. 9. The resulting end-effector trajectory exhibits overshoots similar to those of the nominal case: 0.108 m at each direction change. In response to the larger flexibilities in the manipulator system, oscillations in the time-varying control gains, shown in Fig. 10, are greater than in the nominal case, thereby providing efficient damping of the elastic vibrations while keeping the tracking errors as low as possible. These findings demonstrate that, once the direct fuzzy adaptive algorithm is properly designed under nominal conditions, the results are not significantly sensitive to uncertainties in the system parameters.

As mentioned previously, for most practical applications, the linear joint stiffness assumption is not satisfactory, as several unknown nonlinear effects may affect the end-effector motion. For this reason, it is important to determine the handling capabilities of the controller to unmodeled dynamics. To this end, the fuzzy adaptive composite controller designed for the nominal robot manipulator was applied, without retuning the control parameters and scaling gains, to a more realistic nonlinear joint stiffness model, that includes friction, nonlinear joint stiffness, soft-windup effect, and inertial couplings between motor and link accelerations. More details on the derivation of this nonlinear joint stiffness model, and its parameters can be found in Ref. 6. As shown in Fig. 11, despite the modeling errors, successful trajectory-tracking is achieved by keeping to a minimum the tracking errors along the square trajectory. Figure 12 illustrates that the adaptive control gains reached higher magnitudes in comparison with those previously obtained. This demonstrates that the adaptive fuzzy control scheme copes with modeling errors by adjusting its control parameters to maintain good tracking performance.

In all simulation cases, both components of the proportional and derivative time-varying control gains are bounded by lower limits, given by 5.19 and 6.79 respectively (see Figs. 8, 10, and 12). Indeed, after each subsequent direction switch in the trajectory, the tracking errors tend toward zero, reaching the minimum point on the nonlinear adaptation surface and adaptation curve, which corresponds to 0.0519 for λ_1 and λ_2, and 0.0251 for λ_3 and λ_4. The multiplication of these minimum points by their associated output scaling gains corresponds to the lower bounds of the time-varying control gains observed in Figs. 8, 10, and 12.

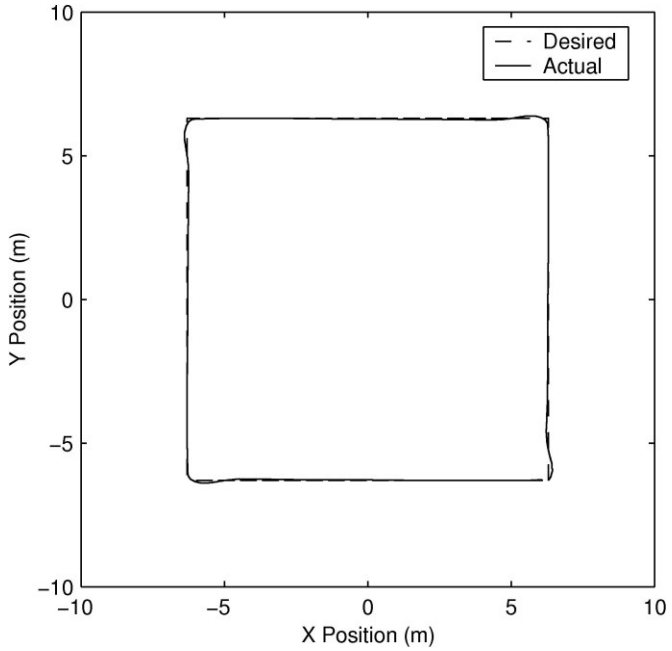

Fig. 7 Trajectory tracking results, linear joint model.

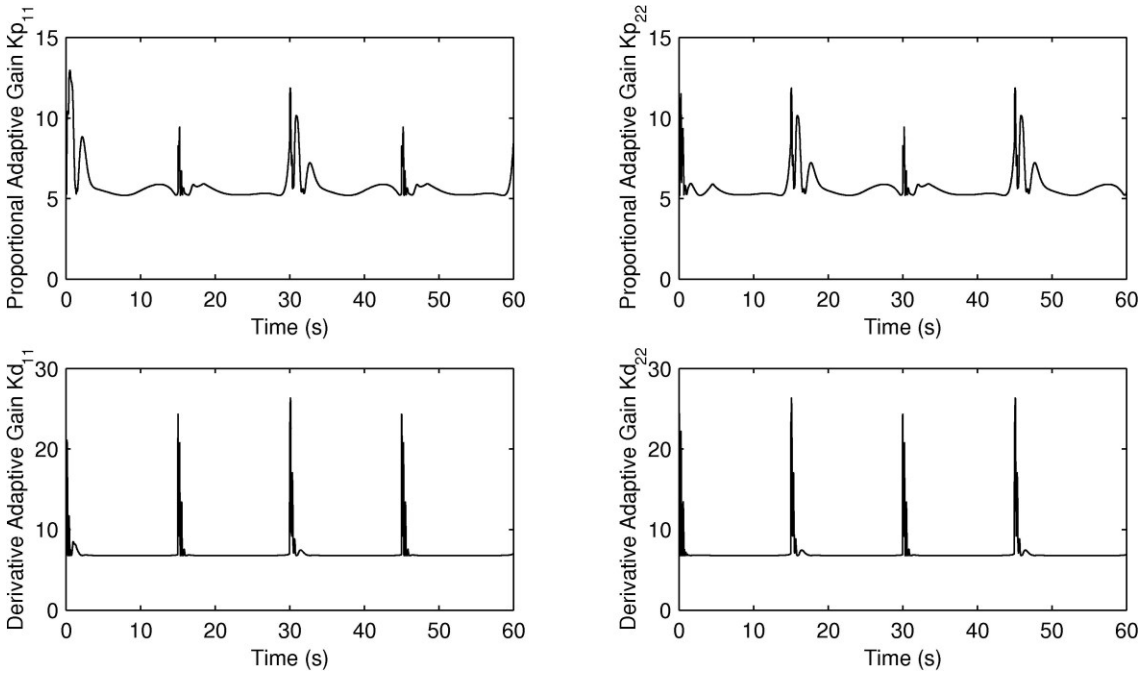

Fig. 8 Control gain adaptation history, linear joint model.

For completeness, and to establish the relative merits of the direct adaptive control strategy compared to existing controllers, numerical simulations were performed with two of the most notable existing flexible-joint control laws: the simple Proportional-Derivative (PD) controller developed by Tomei,[18] and the indirect adaptive composite controller proposed by Spong.[19] The control gains of the PD controller were selected as $\mathbf{K}_p$ = diag[3025] and $\mathbf{K}_d$ = diag[1000] and the indirect adaptive composite controller was designed with $\mathbf{\Lambda}$ = diag[1], $\mathbf{K}_d$ = diag[2], and $\mathbf{K}_v$ = diag[35]. For simplicity, it is assumed that perfect approximation of unknown plant parameters is achieved

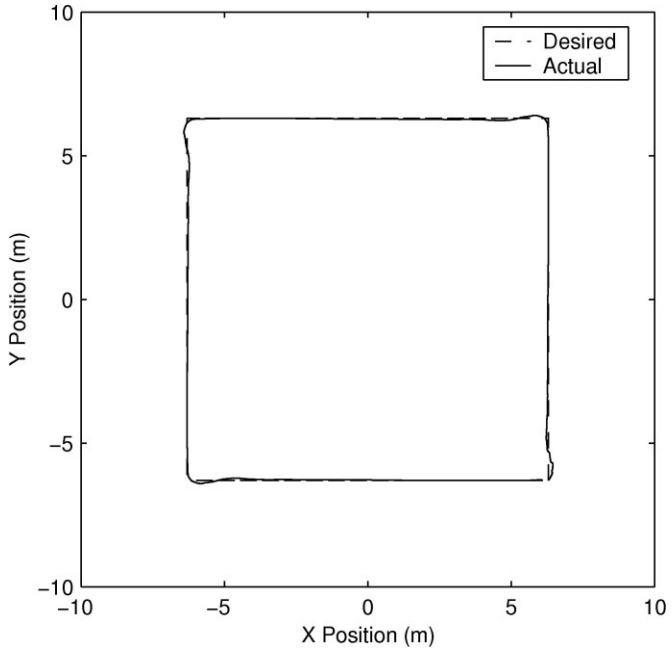

Fig. 9 Trajectory tracking results, uncertain linear joint model (k = diag[200] Nm/rad).

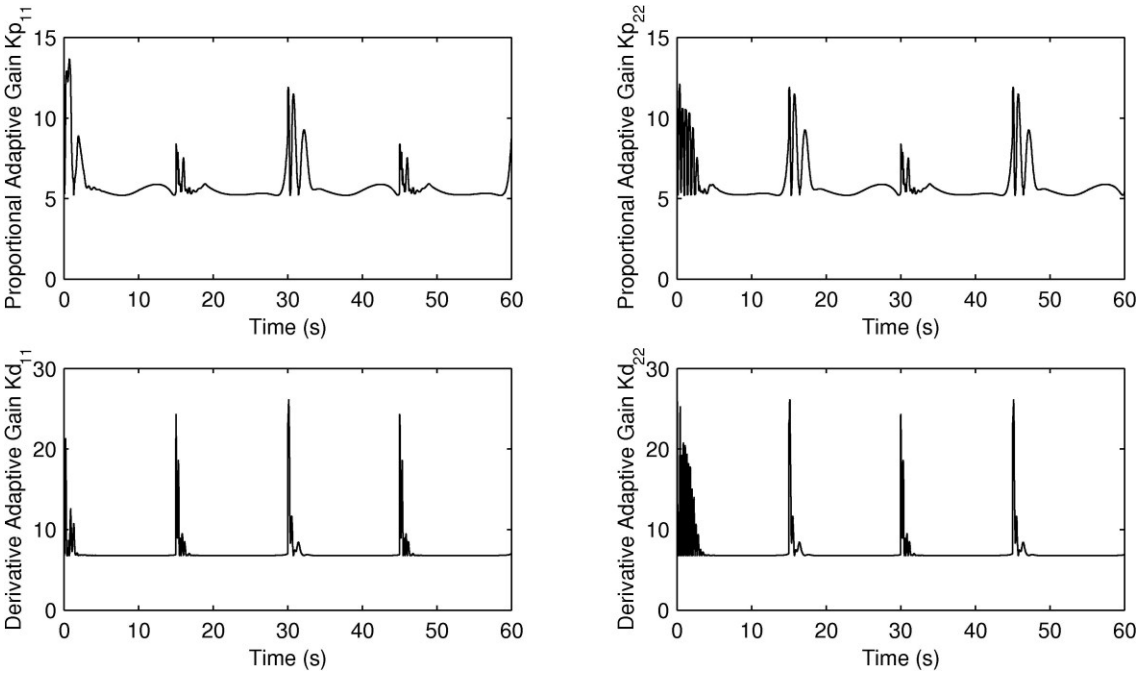

Fig. 10 Control gain adaptation history, uncertain linear joint model (k = diag[200] Nm/rad).

with the indirect adaptive composite controller. In other words, estimates of unknown robot inertia and centrifugal-Coriolis matrices used in the control law were replaced with the actual ones. For more details about these two controllers, the reader is referred to Refs. 18–20. As illustrated in Fig. 13, the PD controller results in significant overshoots at each direction change with sustained oscillations that failed to converge to a straight line along each side of the trajectory, whereas the indirect adaptive composite control scheme provides good tracking results throughout the trajectory, similarly to the direct fuzzy adaptive strategy. The tracking performance of the PD controller is further aggravated when applied to the manipulator with significantly lower joint stiffness, as depicted

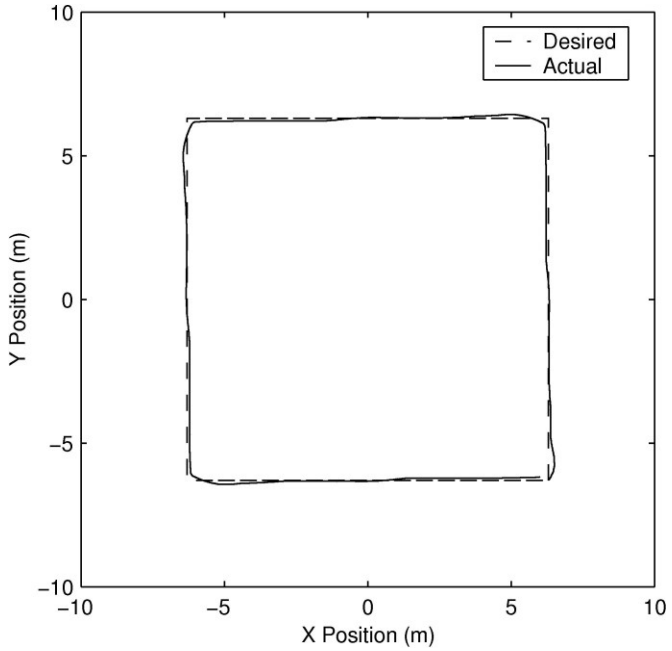

Fig. 11 Trajectory tracking results, nonlinear joint model.

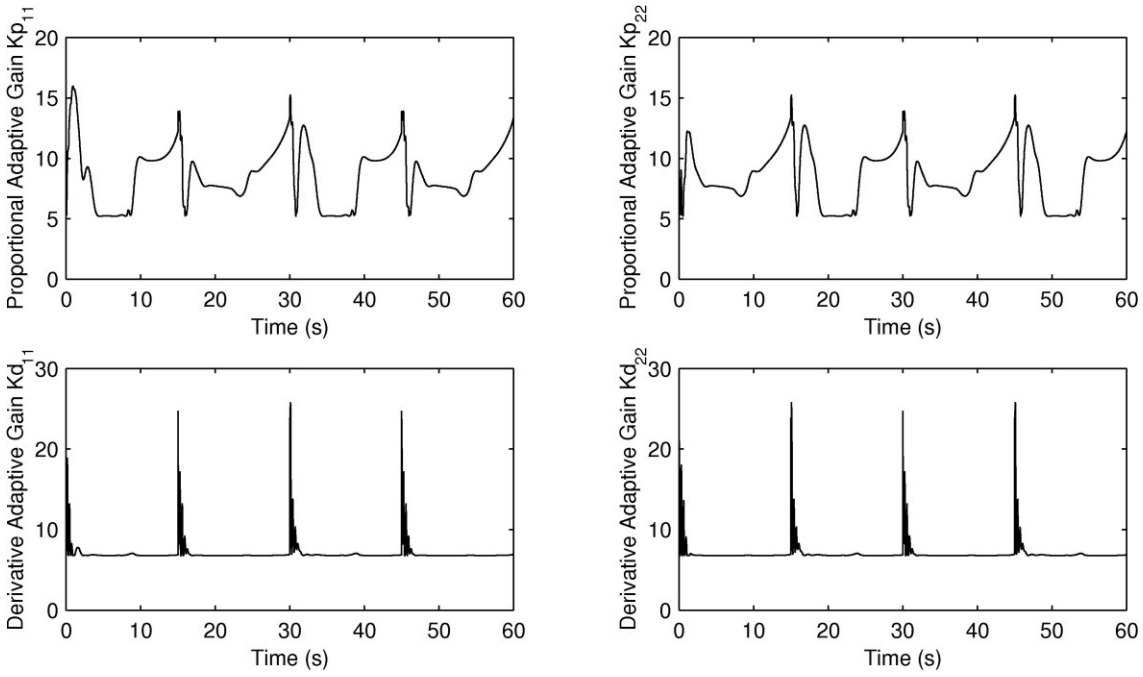

Fig. 12 Control gain adaptation history, nonlinear joint model.

in Fig. 14. However, as with the proposed controller, the indirect adaptive control strategy maintains adequate tracking results despites parametric uncertainties. As anticipated, these results suggest that the fixed-gain PD control strategy cannot cope efficiently with such large uncertainties in the plant parameters. Figure 15 illustrates the limitation of the indirect adaptive controller. Indeed, this controller, as opposed to the one proposed in this paper, is based on good knowledge of the manipulator dynamics model structure. As a consequence, when the same controller tuned with the nominal linear joint model is applied to the nonlinear joint model that includes unmodeled dynamics effects, the indirect adaptive controller does not perform adequately. Contrarily, the end-effector trajectory obtained with PD control strategy exhibits good tracking results, as shown in Fig. 15. This demonstrates the

increased robustness to modeling errors obtained with the model-independent strategies, i.e. the PD controller and the direct fuzzy adaptive controller.

Finally, in comparison with the PD and the indirect adaptive control strategy, these simulation results indicate that the proposed direct fuzzy adaptive composite controller provides significantly improved trajectory tracking results, with an increased robustness to both parametric uncertainties and modeling errors.

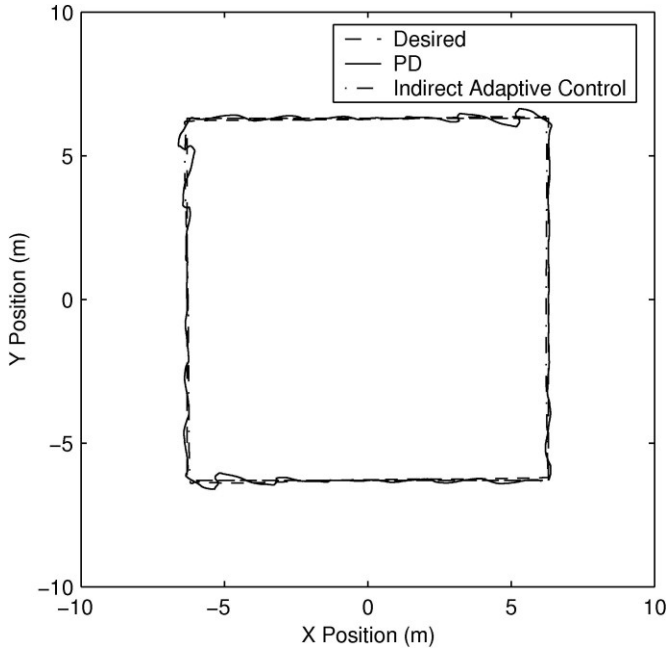

Fig. 13 Trajectory tracking results for the PD and the indirect adaptive controllers, linear joint model.

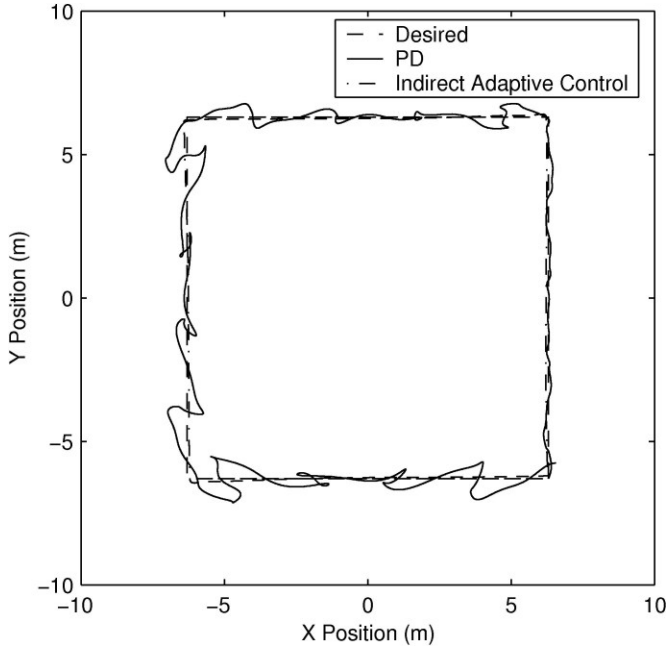

Fig. 14 Trajectory tracking results for the PD and the indirect adaptive controllers, uncertain linear joint model (k = diag[200] Nm/rad).

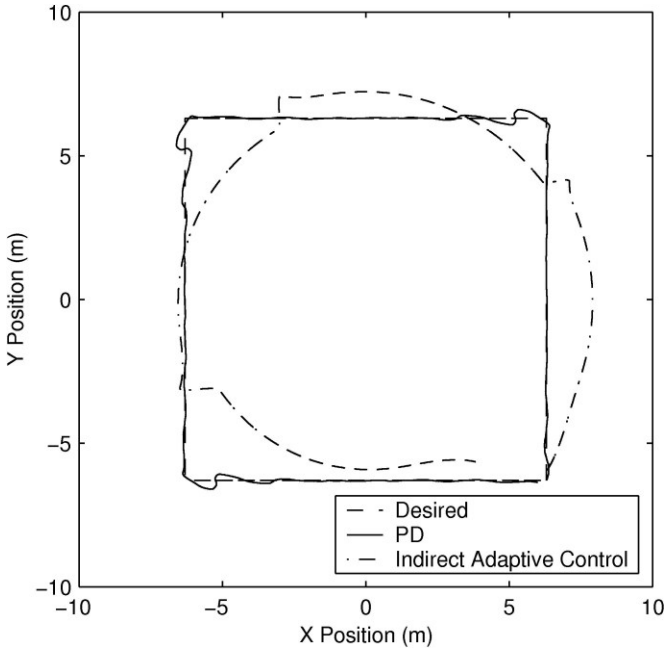

Fig. 15 Trajectory tracking results for the PD and the indirect adaptive controllers, nonlinear joint model.

VI. Conclusion

A novel direct adaptive composite controller was developed for flexible-joint manipulator systems that are subject to parametric uncertainties and modeling errors. The control gain adaptation mechanism of the proposed controller is based on a normalized fuzzy logic system. The fuzzy adaptive system calculates time-varying control parameters in response to tracking errors between the actual plant outputs and the outputs of a reference model, then adapts the control gains to reduce tracking errors. Simulation results obtained from tracking a square trajectory by a manipulator modeled with both the well-known linear joint stiffness model and a newly-developed nonlinear joint stiffness model that is more complex and realistic, established that the proposed control strategy effectively manages significant uncertainties and modeling errors in the plant, by time-varying the control parameters accordingly. Compared to a PD and an indirect adaptive controller, the developed adaptive strategy yields better tracking results along the square trajectory, as well as improved robustness. Future work includes the development of a controller gain adaptation mechanism based on the type-2 fuzzy logic theory, which is known to yield improved tracking performance over conventional fuzzy logic methodologies in situations where uncertainties, modeling errors and disturbances are affecting the plant. Moreover, investigations for a general *n*-DOF manipulator could be pursued.

Acknowledgments

This work was financially supported in part by the J.Y. and E.W. Wong Research Award in Mechanical/Aerospace Engineering from Carleton University, the Canadian Space Agency, the Canadian Armed Forces under the Honorary Colonel S. B. Lerner Memorial Educational Bursary, and the Natural Sciences and Engineering Research Council of Canada under the Alexander Graham Bell Canada Graduate Scholarship CGS D3-374291-2009. The authors are grateful to Dr. Itzhak Barkana for useful discussions on indirect and direct adaptive control methodologies.

References

[1]Khorasani, K., "Nonlinear Feedback Control of Flexible Joint Manipulators: A Single Link Case Study," *IEEE Transactions on Automatic Control*, Vol. 35, No. 10, 1990, pp. 1145–1149.

[2]Palli, G., Melchiorri, C., De Luca, A., "On the Feedback Linearization of Robots with Variable Joint Stiffness," *IEEE International Conference on Robotics and Automation*, Inst. of Electrical and Electronics Engineers, Piscataway, NJ, May 2008, pp. 1753–1759.

[3]Egardt, B., *Stability of Adaptive Controllers*, Springler-Verlag, Berlin, 1979, pp. 1–8.

[4]Cao, Y., and de Silva, C. W., "Dynamic Modeling and Neural-Network Adaptive Control of a Deployable Manipulator System," *Journal of Guidance, Control, and Dynamics*, Vol. 29, No. 1, 2006, pp. 192–194.

[5]Kaufman, H., Barkana, I., and Sobel, K., *Direct Adaptive Control Algorithms: Theory and Applications*, 2nd ed., Communications and Control Engineering Series, Springer, New York, 1997, pp. 5–12.

[6]Ulrich, S., Sasiadek, J. Z., and Barkana, I. "Modeling and Direct Adaptive Control of a Flexible-Joint Manipulator," *Journal of Guidance, Control, and Dynamics*, Vol. 35, No. 1, 2012, pp. 25–39.

[7]Goulet, J. F., de Silva, C. W., Modi, V. J., and Misra, A. K., "Hierarchical Control of a Space-Based Deployable Manipulator Using Fuzzy Logic," *Journal of Guidance, Control, and Dynamics*, Vol. 24, No. 2, 2001, pp. 395–405.

[8]Ahmad, M. A., Raja Ismail, R. M. T., Ramli, M. S., Zawawi, M. A., Hambali, N., and Abd Ghani, N. M., "Vibration Control of Flexible Joint Manipulator using Input Shaping with PD-type Fuzzy Logic Control," *IEEE International Symposium on Industrial Electronics, Inst. of Electrical and Electronics Engineers*, Piscataway, NJ, Oct. 2009, pp. 1184–1189.

[9]Park, C.-W., and Cho, Y. W., "Adaptive Tracking Control of Flexible Joint Manipulator Based on Fuzzy Model Reference Approach," *IEE Proceedings-Control Theory and Applications*, Vol. 150, No. 2, 2003, pp. 198–204.

[10]Weiming, T., Guanrong, C., and Rongde, L., "A Modified Fuzzy PI Controller for a Flexible-Joint Robot Arm with Uncertainties," *Fuzzy Sets and Systems*, Vol. 118, No. 1, 2001, pp. 109–119.

[11]Spong, M. W., "Modeling and Control of Elastic Joint Robots," *Journal of Dynamic Systems, Measurement and Control*, Vol. 109, No. 4, 1987, pp. 310–319.

[12]Spong, M. W., Hutchinson, S., and Vidyasagar, M., *Robot Modeling and Control*, Wiley, New York, 2006, p. 85.

[13]Ott, C., Cartesian Impedance Control of Redundant and Flexible-Joint Robots, *Springer Tracts in Advanced Robotics*, Vol. 49, Springer-Verlag, Berlin Heidelberg, 2008, pp.71–72.

[14]Khalil, H. K., *Nonlinear Systems*, 2nd ed., Prentice–Hall, Upper Saddle River, NJ, 1996, pp. 423–459.

[15]Green, A., and Sasiadek, J. Z., "Adaptive Control of a Flexible Robot Using Fuzzy Logic," *Journal of Guidance, Control, and Dynamics*, Vol. 28, No. 1, 2005, pp. 36–42.

[16]Passino, K. M., and Yurkovich, S., *Fuzzy Control*, Addison–Wesley, Menlo Park, CA, 1998, pp. 63–64, 77–78.

[17]Banerjee, A. K., and Singhose, W., "Command Shaping in Tracking Control of a Two-Link Flexible Robot," *Journal of Guidance, Control, and Dynamics*, Vol. 21, No. 6, 1998, pp. 1012–1015.

[18]Tomei, P., "A Simple PD Controller for Robots with Elastic Joints," *IEEE Transactions on Automatic Control*, Vol. 36, No. 10, 1997, pp. 1208–1213.

[19]Spong, M.W., "Adaptive Control of Flexible Joint Manipulators: Comments on Two Papers,"*Automatica*, Vol. 31, No. 4, 1995, pp. 585–590.

[20]Ulrich, S., and Sasiadek, J. Z., "Control Strategies for Flexible Joint Manipulators," *AIAA Guidance, Navigation, and Control Conference*, Portland, OR, AIAA Paper 2011-6297, Aug. 2011.